

Effect of column loss location on structural response of a generic steel moment resisting frame

Farshad Hashemi Rezvani ^{*1}, Ann E. Jeffers ^{2a}, Behrouz Asgarian ^{3b} and Hamid Reza Ronagh ^{4c}

¹ School of Civil Engineering, University of Queensland, Brisbane, Australia

² Department of Civil and Environmental Engineering, University of Michigan, Ann Arbor, MI, USA

³ Faculty of Civil Engineering, K.N. Toosi University of Technology, Tehran, Iran

⁴ Institute for Infrastructure Engineering, Western Sydney University, Australia

(Received February 17, 2016, Revised January 27, 2017, Accepted July 20, 2017)

Abstract. The effect of column loss location on the structural response of steel moment resisting frames (MRF) is investigated in this study. A series of nonlinear static and dynamic analyses were performed to determine the resistance of a generic frame to an arbitrary column loss and detect the structural members that are susceptible to failure progression beyond that point. Both force-controlled and deformation-controlled actions based on UFC 4-023-03 and ASCE/SEI 41-06 were implemented to define the acceptance criteria for nine APM cases defined in this study. Results revealed that the structural resistance against an arbitrary column loss in the top story is at least 80% smaller than that of the bottom story. In addition, it was found that the dynamic increase factor (DIF) at the failure point is at most 1.13.

Keywords: progressive collapse; failure; vertical incremental dynamic analysis; failure overload factor; pushdown

1. Introduction

During its life, a structure might face an extreme load event resulting in the sudden loss of a column. If there are no alternate paths to redistribute the unbalanced loads within the structure, the initial failure leads to progressive failure of the adjacent members, leading to progressive collapse (ASCE 2005, NIST 2007). General Services Administration (GSA 2003) and Unified Facilities Criteria (UFC 4-023-03) (UFC 2005, 2009) are the primary guidelines for the design of buildings to resist progressive collapse. One particular design approach, termed the Alternate Path Method (APM), is based on the notional removal of columns. According to the GSA and UFC guidelines, a building must have adequate strength to redistribute the loads if one of the building's columns is eliminated (UFC 2005, 2009).

Several investigations have been carried out on progressive collapse behavior of steel frames, especially since the terrorist attack on the World Trade Center (WTC) towers. Research has shown that the dynamic nature of the event should be involved in analyzing a structure and investigating the redistribution of loads following the sudden failure of the column (Kim and Kim 2009). Dynamic amplification of gravity loads has been proposed for static analyses (Kim *et al.* 2009, Tsai and You 2012, Liu

2013, Kheyroddin *et al.* 2014, Song *et al.* 2014) to account for this effect. Different methods are also proposed in order to investigate the robustness of structures subjected to a column loss. An energy-based progressive collapse assessment methodology was proposed by Szyniszewski and Krauthammer (Szyniszewski and Krauthammer 2012), and it was shown that the column deformation energy is a better indicator for structural stability than the maximum dynamic force when the structure is under dynamic loads. Khandelwal and El-Tawil (2011) proposed the use of push-down analysis to assess the robustness of structural frames and to determine the collapse modes of the structure. Liu (Liu 2015) introduced the pull-down analysis via which the capacity of a damaged structure for redistributing loads carried by lost elements was assessed. Li and Hao (2013) examined the substructure method and showed that the method is reliable and efficient for the progressive collapse analysis of structures. Some general conclusions regarding the collapse potential of steel-framed structures can also be gleaned from the literature. For the specific cases investigated by the researchers, it can be said that under column removal scenarios, structures tend to be more susceptible to the loss of an exterior (corner) column (Kim and Kim 2009), and structures with fewer stories (Kim and Kim 2009) and longer spans (Hashemi Rezvani *et al.* 2015) are more vulnerable to collapse. Fu (2009) studied two 20-story buildings with different lateral load carrying systems and reported that vertical displacements of the loss points were larger for a column loss in the fourteenth story compared to that of the first story. Fu (2012) also investigated the effect of consecutive column removals and concluded that in order to mitigate the risk of progressive collapse, beams should be designed with stronger sections

*Corresponding author, Ph.D. Candidate,
E-mail: farshad.hashemi@uq.net.au

^a Ph.D., Associate Professor

^b Ph.D., Professor

^c Ph.D., Professor

in lower floors compared to those in upper floors. Additionally, seismic detailing has been shown to increase a structure's resistance against progressive collapse (Khandelwal *et al.* 2009, Asgarian and Hashemi Rezvani 2012, Hashemi Rezvani and Asgarian 2014).

Although steel Moment Resisting Frames (MRF) are commonly used as the lateral load bearing system in many buildings, the effect of column loss location on their structural response has not been studied completely. Therefore, this research aims to investigate the structural response of a generic steel moment resisting frame to sudden column removal in different locations. In addition, the effect of loss location on the Dynamic Increase Factor (DIF) which relates nonlinear static and dynamic analyses is investigated. Accurate determination of the DIF is of importance since its use can decrease time and effort needed for performing nonlinear element loss analyses.

2. Investigated structure

A generic 10-storey building was investigated to study the effect of column loss location on progressive collapse behavior of moment resisting frames. The plan and elevation view of the building are shown in Figs. 1 and 2. The dead and live loads of 5.5 and 2.0 kN/m², respectively, were used as gravity loads in all stories. The lateral loads were resisted by seismically designed intermediate moment frames, and the building was designed for the Seismic

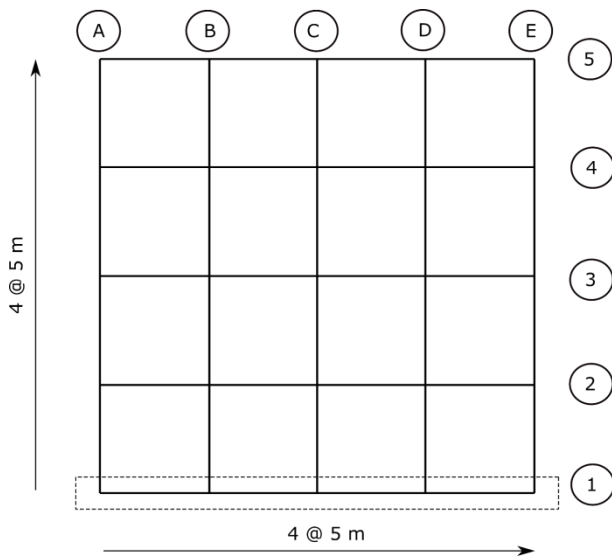


Fig. 1 Plan view of the case study structure

Design Category C according to AISC 360-05 (AISC 2005a) and AISC 341-05 (AISC 2005b). S275 steel with the yield strength of 275 MPa, the ultimate strength of 430 MPa, Young's modulus of 210 GPa and the ultimate strain of 15% was used for structural elements. Table 1 shows the steel sections selected for the studied structure.

3. Modelling of the structure

OpenSEES (Mazzoni *et al.* 2007) was used for analyzing the structure losing its columns. Nonlinear static and dynamic analyses were performed for the exterior frame of the building as shown in Fig. 1 (with dotted lines) and Fig. 2. Steel02 from the material library of OpenSEES with the strain hardening modulus of 0.5% E together with the fatigue material were used to model the steel behavior as shown in Fig. 3 in order to resemble the material properties provided in the previous section. For the beams, and columns, nonlinear displacement-based beam-column elements (dispBeamColumn) were used which employ

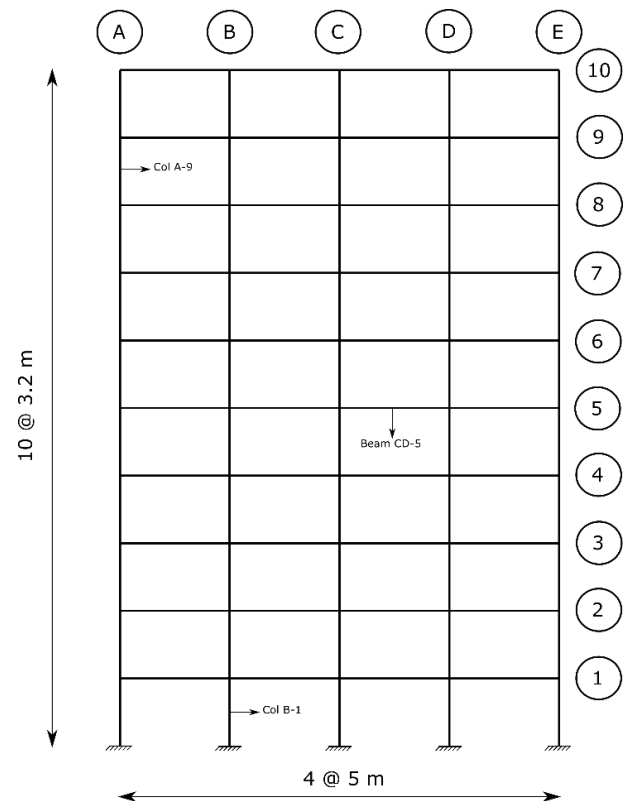


Fig. 2 Elevation view of the case study structure

Table 1 Section sizes of structural members of the case study frame (all dimensions in mm)

Stories	B, C and D axes	A and E axes	Beams
1 and 2	UC356 × 368 × 177	UC356 × 368 × 177	IPE360
3 and 4	UC305 × 305 × 118	UC305 × 305 × 137	IPE360
5 and 6	UC305 × 305 × 118	UC305 × 305 × 118	IPE360
7 and 8	UC254 × 254 × 89	UC254 × 254 × 89	IPE330
9 and 10	UC203 × 203 × 60	UC203 × 203 × 71	IPE270

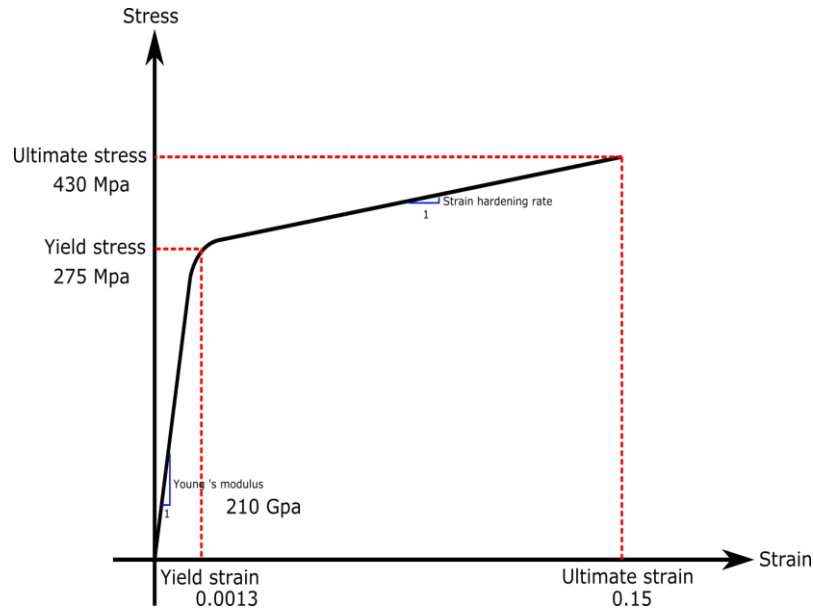


Fig. 3 Material behaviour of Steel02

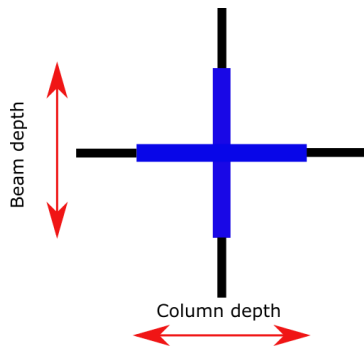


Fig. 4 Structural model at beam-to-column intersection

distributed plasticity approach. An initial mid-span imperfection of $L/300$ was applied to all columns. It was assumed that the beams are connected to the columns by ideally rigid connections. Fig. 4 illustrates the structural model used at the intersection of beams and columns. Since OpenSEES was previously verified and validated (Asgarian and Hashemi Rezvani 2012, Hashemi Rezvani and Asgarian 2012, 2014), no further verification is provided here.

Nine column removal scenarios, termed APM cases, were investigated to investigate the progressive collapse potential and capacity of the structures. Considering the symmetry, three columns, one exterior column and two interior columns (one of which was central), were removed in the first (bottom), fifth (middle), and ninth (top) story of the investigated structure. Table 2 presents the list of APM analysis cases considered together with the member that was removed in each case. The load applied to the structure consisted of the dead (DL) and live (LL) loads according to Eq. (1) (UFC 2009).

$$\text{Applied Load} = 1.2\text{DL} + 0.5\text{LL} \quad (1)$$

3- Acceptance criteria

Nonlinear static and dynamic analyses were performed

Table 2 APM analysis cases

APM case	Removed column	Loss level (floor)	Plan location
1	Col A-1	1	Exterior
2	Col B-1	1	Interior
3	Col C-1	1	Central
4	Col A-5	5	Exterior
5	Col B-5	5	Interior
6	Col C-5	5	Central
7	Col A-9	9	Exterior
8	Col B-9	9	Interior
9	Col C-9	9	Central

to analyze the investigated structure under these APM cases. For nonlinear analyses of steel structures, UFC (UFC 2009) states that except for those connections and elements discussed in the UFC, the modeling parameters and nonlinear acceptance criteria of ASCE 41-06 (ASCE 2007) can be used. These acceptance criteria consist of force-controlled and deformation-controlled actions, where the latter depends on the yield chord rotation (θ_y) of structural members. Chord rotation of a structural member (θ) at each end is the angle between a straight line connecting both ends of the member and a tangent drawn on the deformed shape of the member at that specific end. Assuming a structural member between nodes i and j , this rotation is calculated according to Eq. (2) in which θ_i is the chord rotation at node i , Δ_{ij} is the relative vertical displacement of these two nodes, L is the member length and $\theta_{nodal,i}$ is the nodal rotation at node i . Fig. 5 depicts these parameters.

$$\theta_i = \frac{\Delta_{ij}}{L} - \theta_{nodal,i} \quad (2)$$

UFC states that nonlinear acceptance criteria for

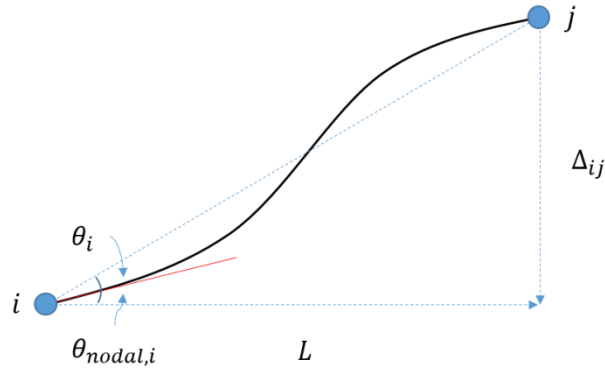


Fig. 5 Calculation of the chord rotation

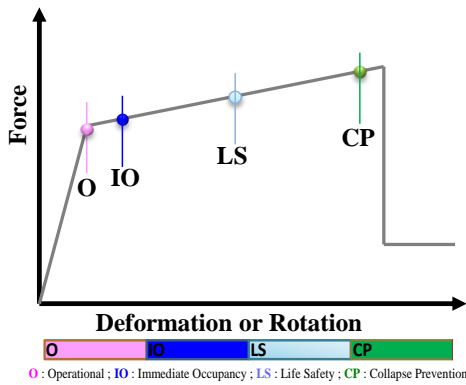


Fig. 6 Conceptual plastic hinge states

structural steel components shall meet the Life Safety condition for primary and secondary elements provided in ASCE 41, except for beams subjected to flexure or flexure plus axial tension for which the Collapse Prevention (CP) condition have to be used. In this study, based on these acceptance criteria, the structural performance of all structural elements is controlled at every stage of the analysis. For the deformation control, the criteria are defined using the Force-Deformation (or chord rotation) diagram as shown schematically in Fig. 6. According to this figure, when the ratio of plastic chord rotation of a structural element (θ_p) to its yield chord rotation exceeds eight, it is said that the structural element has failed (ASCE 2007, UFC 2009). Since in the plastic regions, total chord rotation of a structural element consists of yield and plastic chord rotations, it can be concluded that a structural member is failed if the ratio of its total chord rotation to its yield chord rotation exceeds nine.

Controlling actions of the columns depends on the applied axial load level by which a deformation-controlled action or a force-controlled action should be considered to check the potential of failure occurrence. UFC states that columns under high axial load ($P/P_{CL} > 0.5$) shall be considered force-controlled, with the considered loads (P and M) equal to the maximum loads from the analysis. The $P-M$ interaction equation shall not exceed unity. For $P/P_{CL} \leq 0.5$, the interaction equation shall be used with the moment considered as deformation-controlled and the axial force as force-controlled. The $P-M$ interaction is

determined using Eqs. (3) to (5) (ASCE 2007).

$$\text{For } \frac{P_{UF}}{P_{CL}} < 0.2 : \quad (3)$$

$$DCR = \frac{P_{UF}}{2P_{CL}} + \frac{M_x}{m_x M_{CEx}} + \frac{M_y}{m_y M_{CEy}} \leq 1.0$$

$$\text{For } 0.2 \leq \frac{P_{UF}}{P_{CL}} \leq 0.5 : \quad (4)$$

$$DCR = \frac{P_{UF}}{P_{CL}} + \frac{8}{9} \left[\frac{M_x}{m_x M_{CEx}} + \frac{M_y}{m_y M_{CEy}} \right] \leq 1.0$$

$$\text{For } \frac{P_{UF}}{P_{CL}} > 0.5 : \quad (5)$$

$$DCR = \frac{P_{UF}}{P_{CL}} + \frac{M_{UFx}}{M_{CLx}} + \frac{M_{UFy}}{M_{CLy}} \leq 1.0$$

For the beams, on the other hand, only the deformation-controlled actions are required. This action checks chord rotations of the beams in every step of the analysis to determine whether the acceptance criteria are met. ASCE 41 proposes how to calculate the yield rotation for beam elements as given in Eq. (6) (ASCE 2007). In this equation, Z , F_{ye} , l_b and EI_b are plastic section modulus, expected yield strength, beam length and flexural rigidity of the beam, respectively. However, since ASCE 41, deals with seismic events and assumes that the contra-flexure point occurs at the mid-span of a member, here a series of nonlinear static analyses termed static pushdown analyses were performed to determine yield chord rotation of the beams for each APM case. In this study, the force-controlled action was performed using the expected yield stress while deformation-controlled action was performed using the yield stress.

$$\theta_y = \frac{ZF_{ye}l_b}{6EI_b} \quad (6)$$

4. Analysis method

4.1 Static pushdown analysis

Static pushdown analysis is a nonlinear displacement-controlled analysis in which by increasing the displacement

at the loss point, the gravity load is increased proportionally (Khandelwal and El-Tawil 2011). The analysis continues until reaching the ultimate strain of the material in the cross-sectional fiber elements. However, according to the acceptance criteria, structural elements fail before reaching the ultimate strain. This is shown in the pertinent figures. As a result, load factor versus displacement of the loss point can be drawn which is called static pushdown curve. Load factor is the ratio of the applied gravity load on the structure to the nominal gravity load that according to UFC has to be applied on the structure (Eq. (1)). Moreover, by performing this analysis, it is possible to draw bending moment versus chord rotation of beams in each step of applying vertical displacement of the loss point. This leads to determination of the yield chord rotation of the structural members. According to these curves, drawn for all the beams, and by the acceptance criteria explained previously, it is possible to determine Static Failure Load Factors (SFLFs). SFLF is a load factor at which the failure can occur in other parts of a structure when an arbitrary column is eliminated and is determined in a static pushdown analysis. As another result of such an analysis, it becomes possible to determine which structural element fails prior to others and which APM case is the most critical one. The latter is performed by comparing the associated SFLFs.

4.2 Nonlinear dynamic analysis

Since the sudden loss of a structural element is a dynamic process, performing nonlinear dynamic analyses will provide a better insight into the response. Therefore, in the next step, nonlinear dynamic analyses are performed to determine whether a sudden column loss leads to failure progression or not. Although this does not necessarily indicate the collapse of a structure, it shows its susceptibility to progressive collapse. In this analysis, the gravity loads were linearly increased during five seconds to reach

their final values, and after that, they were kept unchanged for two seconds to avoid excitation of the structure. Although these figures can be selected to assume different value, they were selected as 2 and 5 seconds to be in line with previous studies (Khandelwal *et al.* 2009, Kim and Kim 2009). Once the gravity loads were fully applied after seven seconds, a column related to a predefined APM case was removed suddenly, and afterward the subsequent response of the structure was investigated. Effect of sudden removal of a predefined column could be achieved during the dynamic analysis using “REMOVE” command. To do so, nonlinear dynamic analyses were stopped after seven seconds and followed by removing the predefined column and resuming the analysis. This method not only allows the numerical model to benefit from the stiffness of the removed column before the removal occurs but also makes it possible to form a new stiffness matrix after the removal. These allow modelling sudden column removal as accurately as possible. The simulations were conducted with 5% mass and stiffness proportional damping. In the dynamic analysis for each APM case, the response of the structure is investigated by performing a nonlinear dynamic analysis, and then the analysis results are checked against acceptance criteria to determine whether the failure progression occurs or not. According to the aim of this research which is to investigate the effect of loss location on the relative progressive collapse resistance of a generic moment resisting frame, if a structural element fails following a sudden column loss in a specific APM case, it means that the building is susceptible to progressive collapse in that case. If not, it means that the structure is capable of reaching a static balance after that specific case.

4.3 Vertical incremental dynamic analysis

To determine the structural resistance against a sudden and arbitrary column loss, Vertical Incremental Dynamic

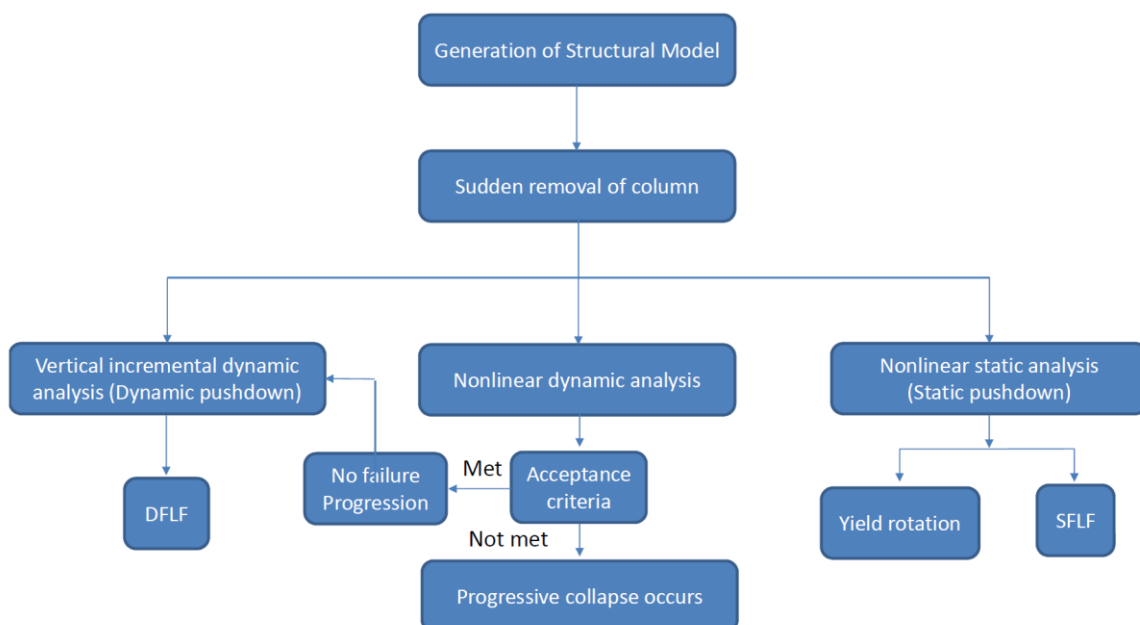


Fig. 7 Analysis method

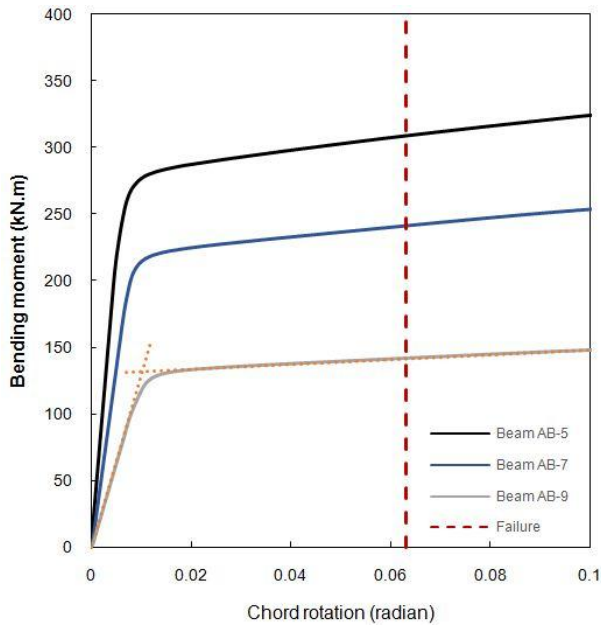


Fig. 8 Bending moment-rotation curves of beams in APM case 4 (Loss of Col A-5)

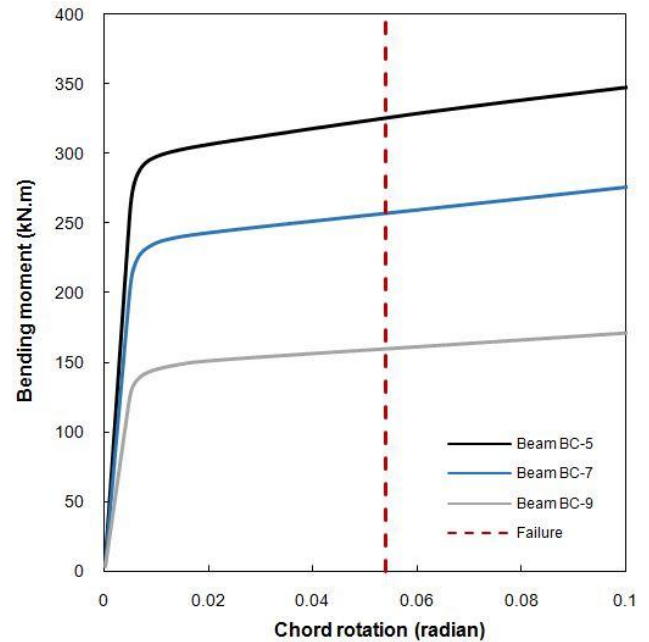


Fig. 9 Bending moment-rotation curves of beams in APM case 5 (Loss of Col B-5)

Analyses (VIDAs), which are similar to incremental dynamic analyses in earthquake engineering, are performed (Khandelwal and El-Tawil 2011, Vamvatsikos and Allin Cornell 2002). VIDA is a dynamic pushdown analysis consisted of a series of nonlinear dynamic analyses in which the applied loads on the structure are incrementally increased. Again, this increase can be reported by a load factor. The main difference between the preliminary nonlinear dynamic analyses and VIDA lays in their objectives. The former determines whether a sudden loss of column leads to failure progression or not while the latter determines structural capacity against failure progression or susceptibility to progressive collapse. This is achieved by comparing the structural response at each load factor with the acceptance criteria. Accordingly, Dynamic Failure Load Factor (DFLF) can be captured. The only difference between SFLF and DFLF is that the latter is computed based on VIDA. By performing VIDA, it is also possible to detect the most critical place where the structure is more

vulnerable to failure progression if it loses a column. Summary of the analysis method is illustrated in Fig. 7.

5. Analyses results and discussion

5.1 Static pushdown analysis

To determine yield chord rotations, bending moment versus chord rotation curves were drawn for all beams in all APM cases. Figs. 8 and 9 illustrate such curves for APM cases 4 (loss of Col A-5) and 5 (loss of Col B-5), respectively. In Fig. 8, as an example, it is shown how the yield rotation of Beam AB-9 is determined in APM case 4. The dotted lines labeled as failure refers to the acceptance criteria as explained previously via which it is possible to determine SFLFs. The failure lines correspond to $\theta_p = 8\theta_y$ for the beam elements which reach this state at a smaller load factor. Therefore, only one failure line is drawn for

Table 3 Yield rotations and SFLF based on static pushdown analyses and ASCE41 equation

APM case	Element	Yield chord rotation (θ_y)		Static failure load factor		Difference (%)
		Pushdown	ASCE41 equation	Pushdown	ASCE41 equation	
1	Beam AB-1	0.007	0.007	1.42	1.42	0.00
2	Beam BC-1	0.006	0.007	1.70	1.73	1.76
3	Beam BC-1	0.006	0.007	1.71	1.74	1.75
4	Beam AB-5	0.007	0.007	1.25	1.25	0.00
5	Beam BC-5	0.006	0.007	1.50	1.52	1.33
6	Beam BC-5	0.006	0.007	1.50	1.53	2.00
7	Beam AB-9	0.008	0.009	0.78	0.79	1.28
8	Beam BC-9	0.007	0.009	0.94	0.97	3.19
9	Beam BC-9	0.007	0.009	0.96	1.00	4.16

each APM case. These figures illustrate the effect of column losses in APM Cases 4 and 5 on the behavior of beam elements and also their yield chord rotations. As is seen, in APM Case 4, the yield chord rotations for beams AB-5, AB-7 and AB-9 are 0.007, 0.008, and 0.010, respectively. In APM Case 5, the yield chord rotation for beams BC-5, BC-7, and BC-9 is 0.006. It depicts that although there is only a beam section at each story level, loss location and axial and flexural stiffness of beam ends can affect the yield chord rotation of beams. Table 3 compares the yield chord rotations determined by performing static pushdown analyses with those obtained according to ASCE41 equation (Eq. (6)). Also, in this table, according to the acceptance criteria, SFLF of critical beams in each APM case is given and as is seen, these yield chord rotations are different. Also, SFLFs determined based on the proposed ASCE41 equation are overestimated in some cases. However, the difference is not significant since it is smaller than 5%. In addition, it can be said that by increasing the loss level the yield chord rotation of beams increases; this is in line with Eq. (6) which shows that by decreasing the section size, the yield chord rotation of beams increases.

5.2 Nonlinear dynamic analysis

A sensitivity analysis was performed for APM case 1 (loss of Col A-1) to determine the time step size which is reliable and efficient for studying the structural behavior. In this analysis, the maximum vertical displacement of the loss point were determined while varying time steps. Fig. 10 depicts the analysis results. According to this figure, it can be seen that there is less than 2% difference between the models with time steps of 0.01 and 0.00125 seconds while the smaller time steps require much longer computation time. Therefore, in the current study, the time step size of $\Delta t = 0.01$ sec was selected.

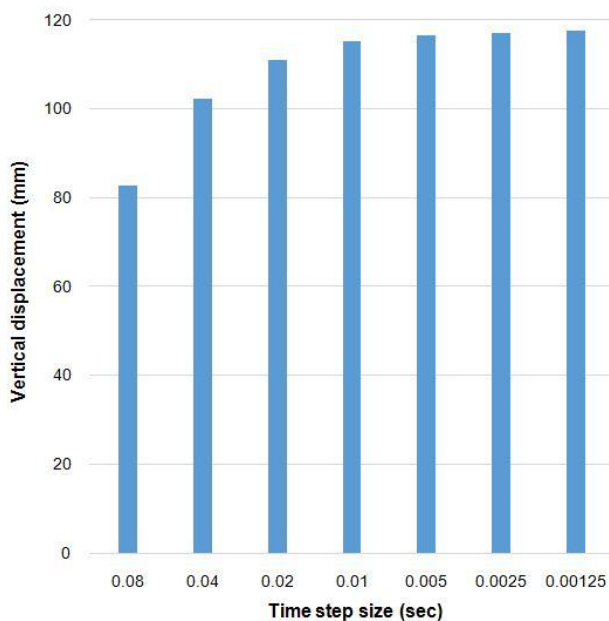


Fig. 10 Effect of time step size on vertical displacement of the loss point in APM case 1 (Loss of Col A-1)

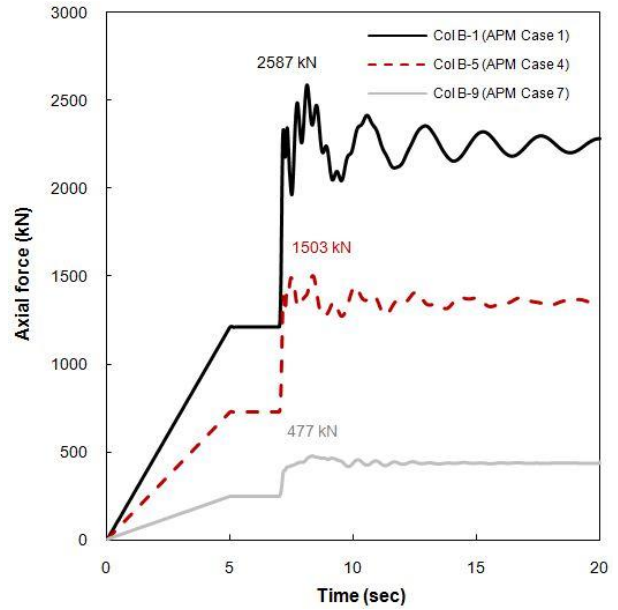


Fig. 11 Response history of axial forces of columns

In Figs. 11 and 12, axial force and bending moments of the critical columns are illustrated, respectively. As shown in Fig. 11, a large redistribution of forces was observed to take place. For example, in the APM case 1 (loss of Col A-1), the axial force of Col-B-1 spiked from 1212 kN to a peak value of 2587 kN before settling down at a steady value of 2281 kN. For this structural member under the same removal case, the bending moment spiked from 18 kN.m to a peak value of 144 kN.m before settling down at a steady value of 111 kN.m. However, the axial force and bending moment capacities of Col-B-1 are 5400 kN and 763 kN.m, respectively according to ASCE 41-06 (ASCE 2007). They are substantially more than the peak value

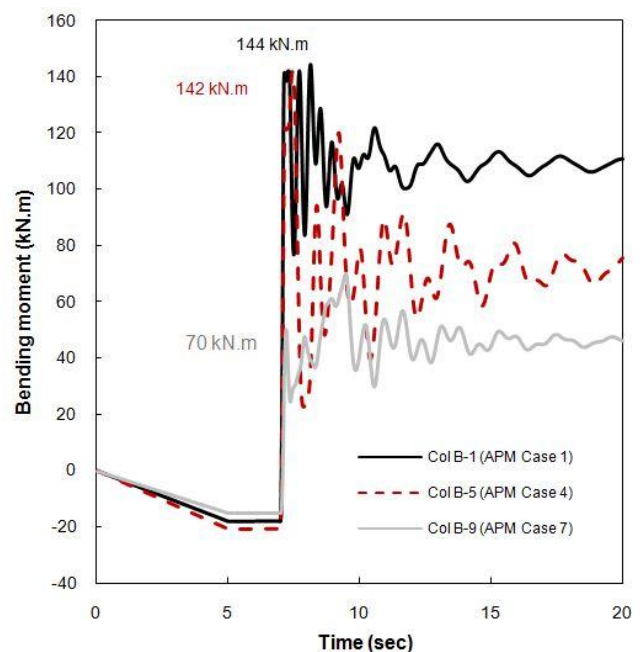


Fig. 12 Response history of bending moment of columns

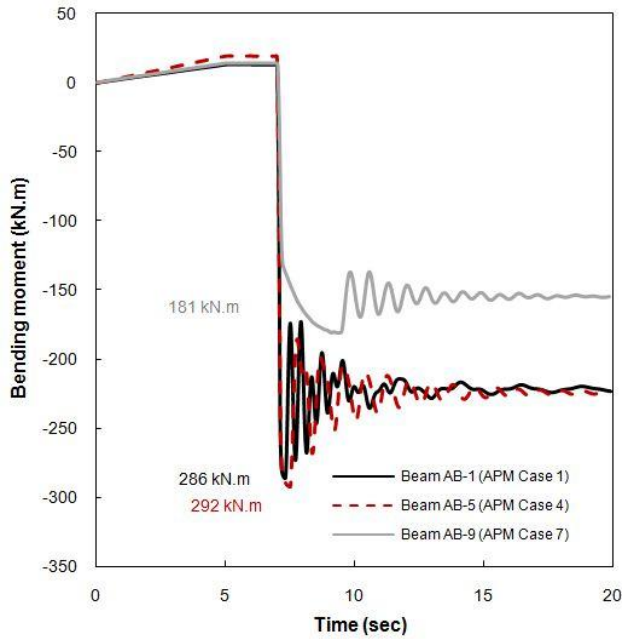


Fig. 13 Response history of bending moment of beams

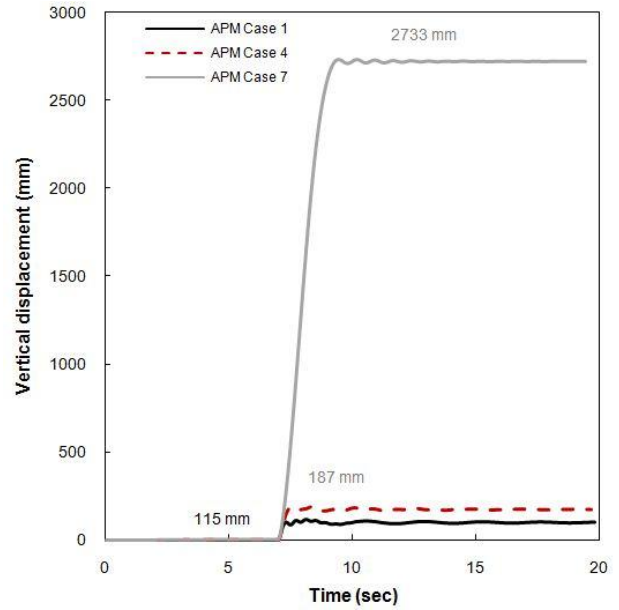


Fig. 14 Vertical displacement of loss point

computed in this column which implies that the column will not be overloaded. Fig. 13 depicts the response history of critical beams in APM cases 1, 4, and 7 (loss of exterior columns). As shown, in the APM case 1, for example, the bending moment of Beam AB-1 spiked from 13 kN.m to a peak value of 286 kN.m before settling down at a steady value of 223 kN.m.

The previous description of structural behaviour only focused on force-controlled actions but, as mentioned previously, to check the robustness of the studied frame the deformation-controlled actions also should be followed. Accordingly, vertical displacements of the removal points pertinent to exterior column losses are shown in Fig. 14. As per this figure, it is evident that the vertical displacements dramatically increase when the columns are suddenly removed. For example, vertical displacement of the removal point in APM case 7 (loss of Col A-9) increases from 4 mm to a peak value of 2,733 mm and then dampens to a value of 2,722 m. This was followed by reaching the ultimate strain of the material which according to the acceptance criteria,

implies that the beam element connected to this point has failed before reaching this large displacement. As shown, the vertical displacement of the loss point drastically increases as the loss level increases. The lower axial and flexural stiffness of structural elements in the upper stories explains this behaviour.

Based on the yield chord rotations determined according to the static pushdown analyses, Figs. 15 and 16 depict response history of the ratio of plastic chord rotation to yield chord rotation of beams. As is evident, these ratios dramatically increase when columns are removed. Comparing these curves with the acceptance criteria labelled failure, it can be seen that loss of an arbitrary column in the ninth story leads to failure progression and implies that the frame is susceptible to progressive collapse. Summary of the dynamic analyses is given in Table 4. According to this table, it can be inferred that failure of beams occurs prior to failure of columns in the top story. Fig. 17 shows the location of plastic hinges formed because of predefined column losses (shown with dash lines) in the APM cases 1 (loss of Col A-1) and 7 (loss of Col A-9)

Table 4 Critical DCRs and rotation ratios

APM case	DCR		θ_p/θ_y		θ_y	
	Value	Element	Value	Failure limit		
1	0.65	Col B-1	1.41	8	Beam AB-1	0.007
2	0.37	Col A-1	0.71	8	Beam BC-1	0.006
3	0.47	Col D-1	0.72	8	Beam BC-1	0.006
4	0.70	Col B-5	3.00	8	Beam AB-5	0.007
5	0.35	Col A-5	1.19	8	Beam BC-5	0.006
6	0.46	Col D-5	1.19	8	Beam BC-5	0.006
7	0.54	Col B-9	61.76	8	Beam AB-9	0.008
8	1.01	Col A-9	25.80	8	Beam BC-9	0.007
9	0.66	Col D-9	18.97	8	Beam BC-9	0.007

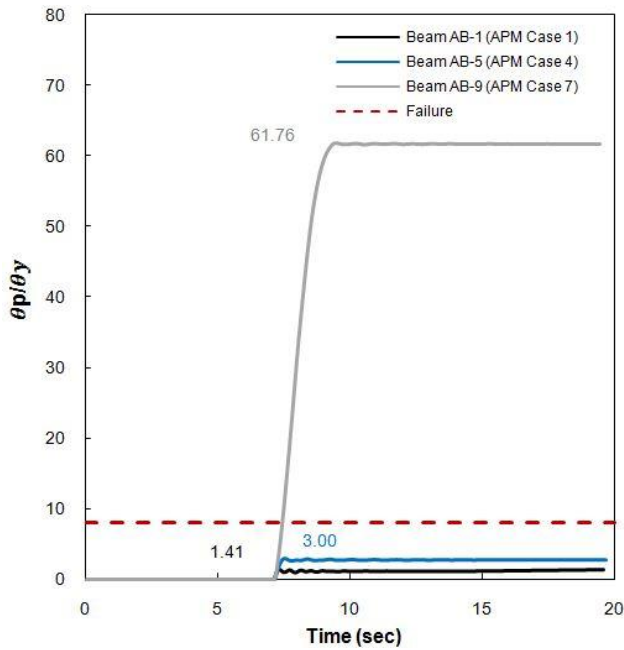


Fig. 15 Plastic rotation to yield rotation ratio of beams – loss of exterior columns

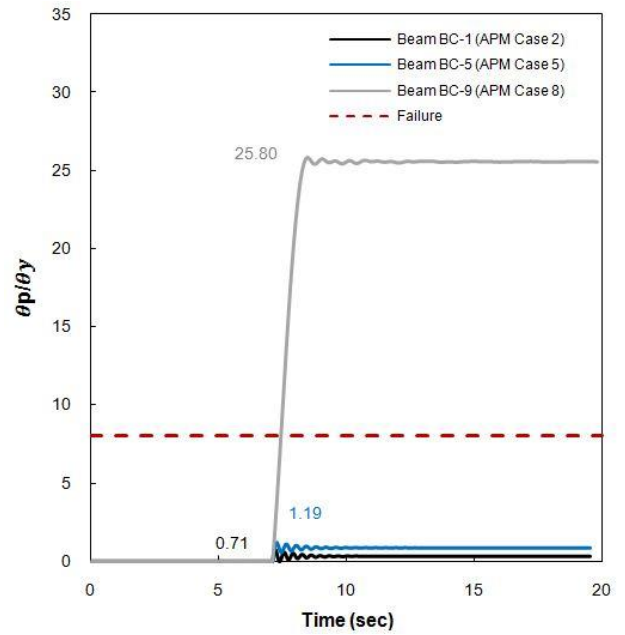


Fig. 16 Plastic rotation to yield rotation ratio of beams – loss of interior columns

together with the ratio of plastic chord rotation to the yield rotation of each beam.

5.3 Vertical incremental dynamic analysis

VIDA aims to determine the structural resistance against an arbitrary column loss. Fig. 18 illustrates how the load factor affects response history of the ratio of plastic chord

rotation to yield chord rotation of Beam BC-5 in APM case 5 (loss of Col B-5). After performing nonlinear dynamic analyses for a specific load factor, both force-controlled and deformation-controlled actions were evaluated to check whether structural elements meet the acceptance criteria or not. In each APM case the smallest load factor which causes failure progression is reported as the DFLF. It is worth noting that according to Table 5, DFLF of the last three

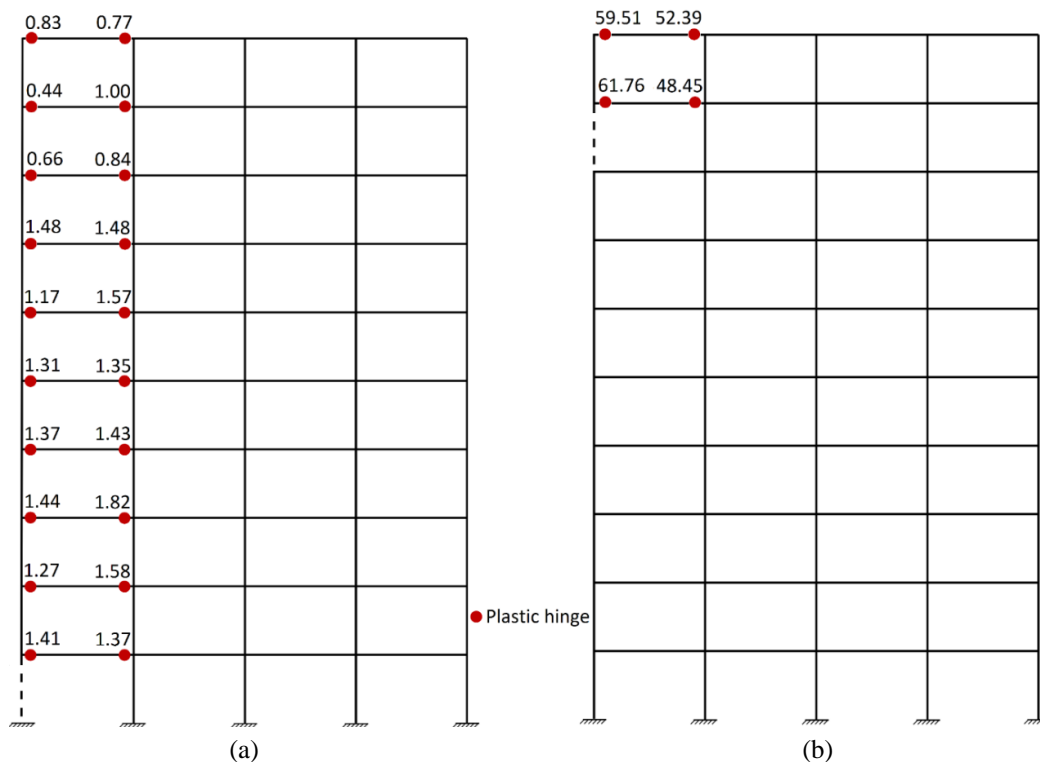


Fig. 17 Plastic hinge status (a) APM case 1; (b) APM case 7

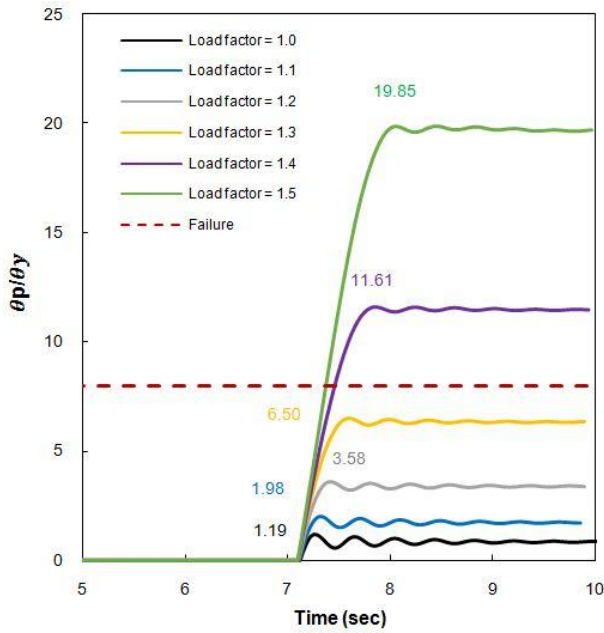


Fig. 18 Plastic rotation to yield rotation ratio of Beam BC-5 in APM Case 5 (Loss of Col B-5)

APM cases which are associated with column losses in the top story are essentially less than unity. In these three cases, acceptance criteria are not met.

Fig. 19 depicts DCRs of the critical members for the first six investigated APM cases. Because the preliminary dynamic analyses did not show the collapse of the structure for these cases, DCRs are smaller than unity at the load factor of unity. Figs. 20 to 22 show static and dynamic (VIDA) pushdown analyses results for the critical beams in each APM case. It is evident that for a specific load factor, dynamic analysis exhibits larger deformation. According to these figures, it is possible to determine SFLFs and DFLFs. Based on these results, Fig. 23 illustrates the deformation-controlled action by presenting the ratio of maximum plastic chord rotation to yield chord rotation of critical beams for the investigated APM cases. Like DCRs, when the load factor is equal to one, the ratio of peak plastic

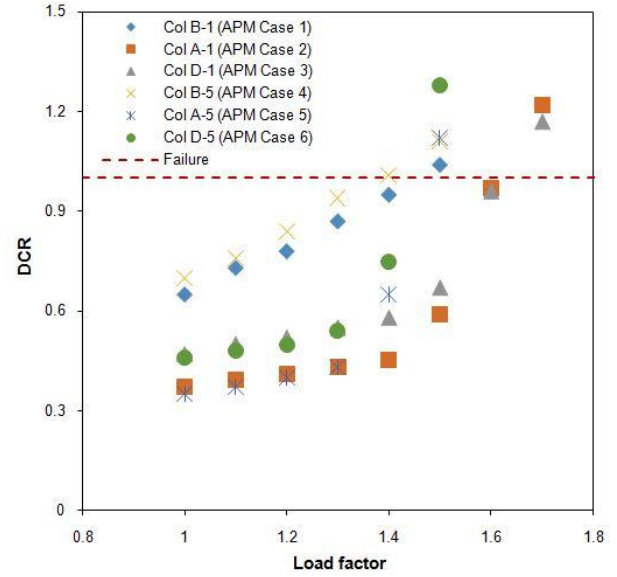


Fig. 19 DCRs for critical structural members

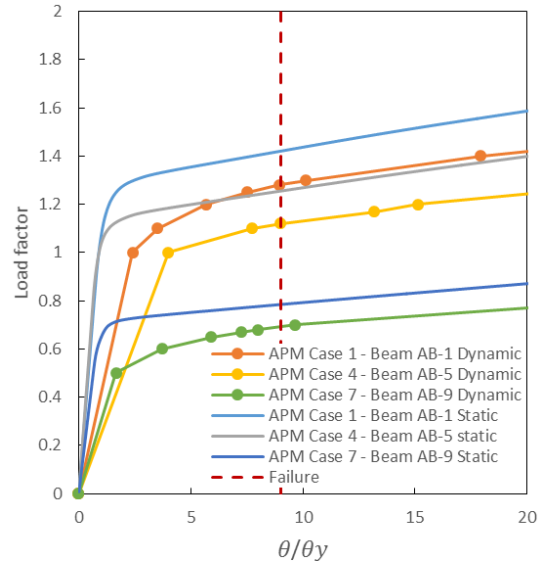


Fig. 20 Static pushdown and VIDA for the column losses in the bottom story

Table 5 Static and dynamic failure load factors

APM case	Static pushdown analysis		Vertical incremental dynamic analysis (dynamic pushdown analysis)			
	Deformation-controlled action		Force-controlled action		Deformation-controlled action	
	SFLF	Element	DFLF	Element	DFLF	Element
1	1.42	Beam AB-1	1.46	Col B-1	1.28	Beam AB-1
2	1.70	Beam BC-1	1.61	Col A-1	1.53	Beam BC-1
3	1.71	Beam BC-1	1.62	Col D-1	1.53	Beam BC-1
4	1.25	Beam AB-5	1.39	Col B-5	1.12	Beam AB-5
5	1.50	Beam BC-5	1.47	Col A-6	1.34	Beam BC-5
6	1.50	Beam BC-5	1.45	Col D-5	1.34	Beam BC-5
7	0.78	Beam AB-9	1.37	Col B-9	0.69	Beam AB-9
8	0.94	Beam BC-9	1.00	Col A-9	0.84	Beam BC-9
9	0.96	Beam BC-9	1.42	Col D-9	0.85	Beam BC-9

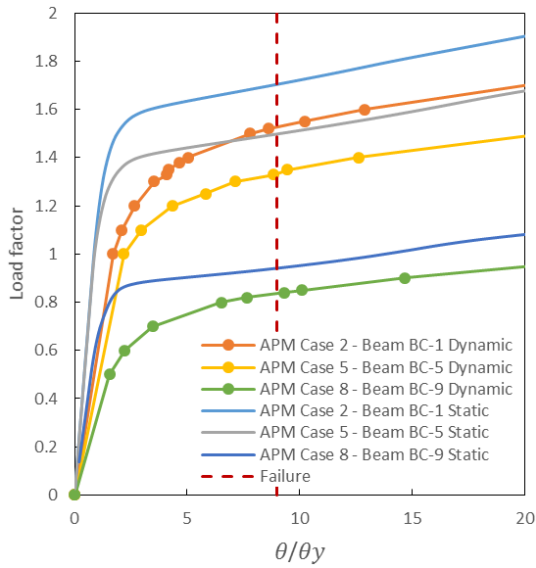


Fig. 21 Static pushdown and VIDA for the column losses in the middle story

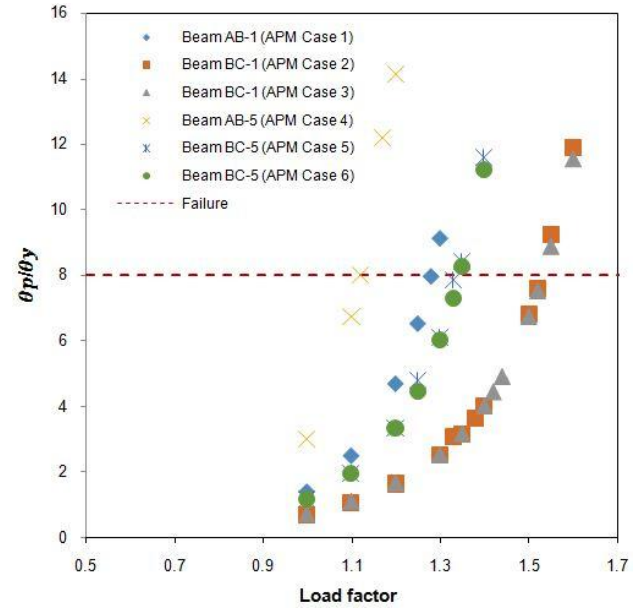


Fig. 23 Plastic rotation to yield rotation ratios

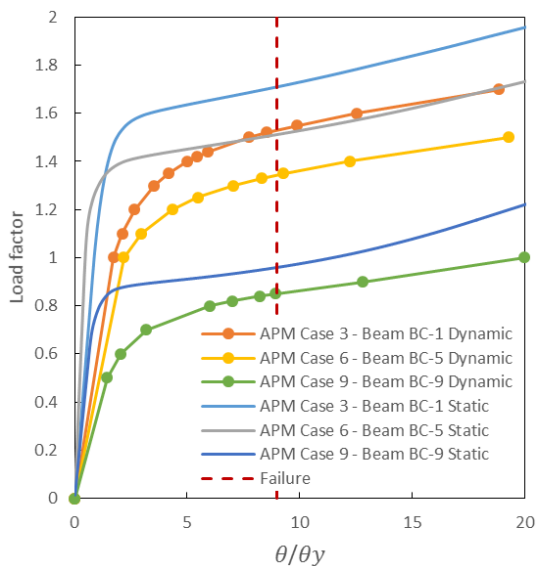


Fig. 22 Static pushdown and VIDA for the column losses in the top story

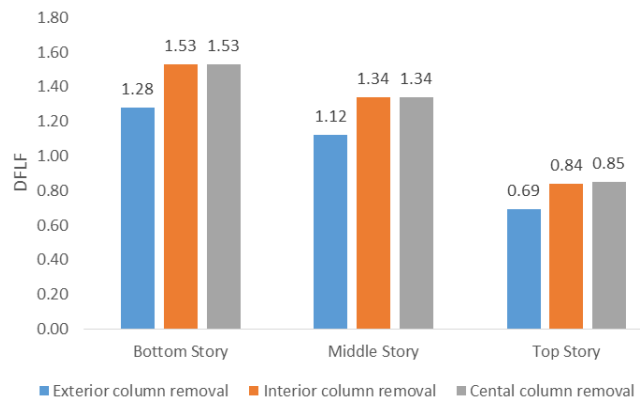


Fig. 24 Dynamic Failure Load Factors (DFLFs)

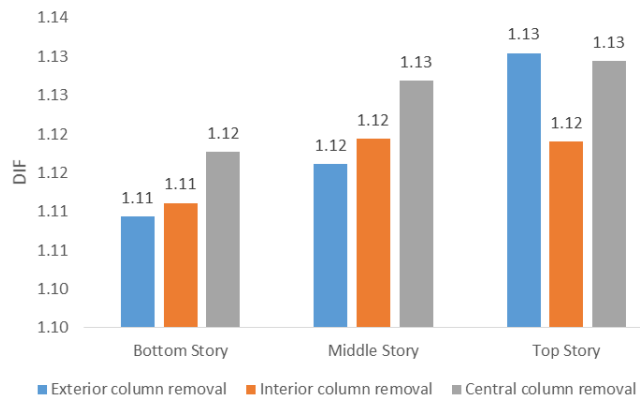


Fig. 25 Dynamic increase factors at the failure point

chord rotation to yield chord rotation meets the acceptance criteria meaning that the structure does not exhibit susceptibility to progressive collapse even in the deformation-controlled action.

SFLFs and DFLFs for forced-controlled and deformation-controlled actions are given in Table 5. Noting that loss of a column in the top story leads to progressive collapse, it is evident that the failure load factors of both force-controlled and deformation-controlled actions decrease as the loss level increases. According to the results, Fig. 24 illustrates the smallest DFLF for each APM case which shows the structural resistance against them. It is obvious that the DFLFs decrease while the loss level increases. This means that as the loss level increases the potential for the occurrence of progressive collapse increases. In addition, it

is shown that sudden loss of exterior columns leads to more critical situations for failure progression compared to loss of interior or central columns. Also, it can be said that the deformation-controlled action associated to the VIDA reports the smallest DFLF in each case. This figure also

depicts that loss location has a great influence on the resistance of a steel MRF, i.e., there is at least 80% difference between DFLFs determined for a column loss in the bottom and top stories.

5.4 Dynamic increase factor at the failure point

As progressive collapse is a dynamic and nonlinear event, the applied load for the static procedures require the use of magnification factors, which approximately account for inertial and nonlinear effects. For both linear static and nonlinear static analyses, UFC 4-023-03 (UFC 2005) and GSA guidelines use a load multiplier of 2.0. However, because of problems identified with the use of a fixed factor of 2, in the latest edition of UFC 4-023-03, two different magnification factors, namely the load increase factor (LIF) and dynamic increase factor (DIF), were proposed to consider the dynamic effect in linear and nonlinear static analysis, respectively (UFC 2009). The LIF is intended to account for the material nonlinearity and the dynamic effect, while the DIF is only responsible for the latter. For a steel frame, UFC recommended DIF is as given in Eq. (7) (UFC 2009).

$$DIF = 1.08 + \frac{0.76}{\frac{\theta_p}{\theta_y} + 0.83} \quad (7)$$

Using the results of nonlinear static and dynamic (VIDA) analyses, a DIF associated with the failure of first structural element is defined ($DIF_{failure}$). This factor is calculated for the investigated APM cases. This is done according to Eq. (8) and the results provided in Table 5. The ratio of the SFLF to the DFLF is important since it gives insight to the effect of loss location on the DIF and interconnects nonlinear static and dynamic analyses results.

$$DIF_{failure} = \frac{SFLF}{DFLF} \quad (8)$$

These DIFs are depicted in Fig. 24. As is seen, by increasing the loss level, the increases in this factor remain below 1.13 for all loss locations. Therefore, without performing vertical incremental dynamic analysis which is computationally prohibitive, it is possible to estimate the dynamic failure load factor using the static one determined in the pushdown analysis.

6. Conclusions

In this study, the effect of column loss location on progressive collapse behaviour and resistance of a generic steel moment resisting frame was investigated. For this purpose, a ten-story steel MRF was studied against nine loss scenarios located in different locations in the first, fifth and ninth stories. Nonlinear static and dynamic analyses were performed to study the behaviour of this structure. In this study, both force-controlled and deformation-controlled actions were implemented to determine the residual strength of the studied frame. Firstly, pushdown analyses were performed to determine the yield chord rotation of beams.

Results led to the following conclusions:

- Although the yield chord rotations determined according to pushdown analyses are different from those obtained using the ASCE41 equation, this difference only affects static failure load factors by less than 5%.
- In the investigated generic frame, the loss of an arbitrary column in the top story initiates the failure progression in beams. It was also shown that increasing the loss level decreases the frame's resistance to progressive collapse.
- Column loss location has a great influence on the resistance of steel MRFs to progressive collapse. In the studied frame, there was 80% difference between the resistance of the frame for losses in the bottom and top story. Therefore, for the critical buildings, it is recommended to increase the size of structural members and accordingly, to strengthen the beam-to-column connections to mitigate the risk of progressive collapse in upper stories.
- A dynamic increase factor was defined in this study which was calculated based on nonlinear static and dynamic (VIDA) analyses at the failure point. It was shown that by increasing the loss level, this factor increases and for all loss locations, DIF is at most 13%. Therefore, using this factor, it is possible to estimate the dynamic failure load factor based on the static one determined in pushdown analysis without performing vertical incremental dynamic analysis which is computationally prohibitive.

References

- American Institute of Steel Construction (2005a), AISC 360-05, Specification for Structural Steel Buildings; Chicago, IL, USA.
- American Institute of Steel Construction (2005b), AISC 341-05, Seismic provisions for structural steel buildings; Chicago, IL, USA.
- American Society of Civil Engineers (2005), ASCE 7-05, minimum design loads for buildings and other structures; New York, NY, USA.
- American Society of Civil Engineers (2007), ASCE/SEI 41-06, Seismic Rehabilitation of Existing Buildings, Reston, VA, USA.
- Asgarian, B. and Hashemi Rezvani, F. (2012), "Progressive collapse analysis of concentrically braced frames through EPCA algorithm", *J. Construct. Steel Res.*, **70**, 127-136.
- Fu, F. (2009), "Progressive collapse analysis of high-rise building with 3-D finite element modeling method", *J. Construct. Steel Res.*, **65**(6), 1269-1278.
- Fu, F. (2012), "Response of a multi-storey steel composite building with concentric bracing under consecutive column removal scenarios", *J. Construct. Steel Res.*, **70**, 115-126.
- GSA (2003), Progressive collapse analysis and design guidelines for new federal office buildings and major modernization projects; U.S. General Service Administration (U.S. GSA), Washington DC, USA.
- Hashemi Rezvani, F. and Asgarian, B. (2012), "Element loss analysis of concentrically braced frames considering structural performance criteria", *Steel Compos. Struct., Int. J.*, **12**(3), 231-248.
- Hashemi Rezvani, F. and Asgarian, B. (2014), "Effect of seismic design level on safety against progressive collapse of

- concentrically braced frames “, *Steel Compos. Struct., Int. J.*, **16**(2), 135-156.
- Hashemi Rezvani, F., Yousefi, A.M. and Ronagh, H.R. (2015), “Effect of span length on progressive collapse behaviour of steel moment resisting frames”, *Structures*, **3**, 81-89.
- Khandelwal, K. and El-Tawil, S. (2011), “Pushdown resistance as a measure of robustness in progressive collapse analysis”, *Eng. Struct.*, **33**(9), 2653-2661.
- Khandelwal, K., El-Tawil, S. and Sadek, F. (2009), “Progressive collapse analysis of seismically designed steel braced frames”, *J. Construct. Steel Res.*, **65**(3), 699-708.
- Kheyroddin, A., Gerami, M. and Mehrabi, F. (2014), “Assessment of the dynamic effect of steel frame due to sudden middle column loss”, *Struct. Des. Tall Special Build.*, **23**(5), 392-402.
- Kim, J. and Kim, T. (2009), “Assessment of progressive collapse-resisting capacity of steel moment frames”, *J. Construct. Steel Res.*, **65**(1), 169-179.
- Kim, H.S., Kim, J. and An, D.W. (2009), “Development of integrated system for progressive collapse analysis of building structures considering dynamic effects”, *Adv. Eng. Software*, **40**(1), 1-8.
- Li, J. and Hao, H. (2013), “Numerical study of structural progressive collapse using substructure technique”, *Eng. Struct.*, **52**, 101-113.
- Liu, M. (2013), “A new dynamic increase factor for nonlinear static alternate path analysis of building frames against progressive collapse”, *Eng. Struct.*, **48**, 666-673.
- Liu, M. (2015), “Pulldown Analysis for Progressive Collapse Assessment”, *J. Perform. Construct. Facil.*, **29**(1), 04014027.
- Mazzoni, S., McKenna, F., Scott, M.H. and Fenves, G.L. (2007), OpenSees command Language manual.
- National Institute of Standard and Technology (2007), NISTIR 7396, Best practices for reducing the potential for progressive collapse in buildings; Technology administration, U.S. Department of Commerce.
- Song, B.I., Giriunas, K.A. and Sezen, H. (2014), “Progressive collapse testing and analysis of a steel frame building”, *J. Construct. Steel Res.*, **94**, 76-83.
- Szyniszewski, S. and Krauthammer, T. (2012), “Energy flow in progressive collapse of steel framed buildings”, *Eng. Struct.*, **42**, 142-153.
- Tsai, M.-H. and You, Z.-K. (2012), “Experimental evaluation of inelastic dynamic amplification factors for progressive collapse analysis under sudden support loss”, *Mech. Res. Commun.*, **40**, 56-62.
- Unified Facilities Criteria (2005), UFC 4-023-3, Design of buildings to resist progressive collapse; Department of Defense, Washington DC, USA.
- Unified Facilities Criteria (2009), UFC 4-023-3, Design of buildings to resist progressive collapse; Department of Defense, Washington DC, USA.
- Vamvatsikos, D. and Allin Cornell, C. (2002), “Incremental dynamic analysis”, *Earthq. Eng. Struct. Dyn.*, **31**(3), 491-514.

BU

List of symbols

Δ_{ij}	Relative vertical displacement of beam ends
θ	Chord rotation
θ_i	Chord rotation of node i
θ_p	Plastic chord rotation
θ_y	Yield chord rotation
$\theta_{nodal,i}$	Nodal rotation of node i
EI_b	Flexural rigidity of beam
DCR	Demand over capacity ratio
$DFLF$	Dynamic failure load factor
$DIF_{failure}$	Dynamic increase factor at failure
DL	Dead load
E	Modulus of elasticity
F_{ye}	Expected yield strength
P	Axial force
P_{CL}	Axial compression capacity
P_{UF}	Axial force in the member
M_{CEX}	Expected bending strength of the column for the x-axis
M_{CEY}	Expected bending strength of the column for the y-axis
M_{CLX}	Lower-bound flexural strength of the member about the x-axis
M_{CLY}	Lower-bound flexural strength of the member about the y-axis
M_x	Bending moment in the member for the x-axis
M_y	Bending moment in the member for the y-axis
m_x	Value of m for the column bending about the x-axis
m_y	Value of m for the column bending about the y-axis
M_{UFx}	Bending moment in the member about the x-axis
M_{UFy}	Bending moment in the member about the y-axis
L	Member length
l_b	Beam length
LL	Live load
$SFLF$	Static failure load factor
Z	Plastic section modulus